NJC

PAPER

View Article Online
View Journal | View Issue

Cite this: *New J. Chem.*, 2025, **49**, 8494

Cyclometalated platinum(II) complex-based soft salt with multistimuli-responsive properties†

Alexandre Rico,[a] Pascal Le Poul,[a] Antonin Lyčka,[b] Julián Rodríguez-López,[c] Sylvain Achelle[a] and Sébastien Gauthier*[a]

Received 28th March 2025,
Accepted 28th April 2025

DOI: 10.1039/d5nj01402f

rsc.li/njc

A soft salt, **S**, comprising two oppositely charged platinum(II) complexes, ($[Pt(C_{F_2}\text{^}N)(en)]^+$ and $[Pt(C_{Ph_2}\text{^}N)(CN)_2]^-$), was synthesized and characterized. Compound **S** exhibits photoluminescence in DMSO solution, emitting at 558 nm upon excitation at 414 nm, with a quantum yield of 0.49. In the solid state, when dispersed in a KBr matrix, a broad emission band centered at 658 nm is observed. The cationic and anionic components of **S** interact through electrostatic and van der Waals forces, leading to pronounced modifications of their luminescent behavior compared to their isolated counterparts. These include vapochromic responses, reversible photoluminescence quenching upon exposure to acid vapors, and thermally induced luminescence enhancement.

Introduction

Stimuli-responsive materials are of great interest for applications in photocatalysis,[1] displays,[2] data storage,[3] sensing, bioimaging,[4] and security.[5] External stimuli such as solvents,[6] temperature,[7] pressure,[8,9] light,[10] pH,[11] or electric fields[12] can trigger stereoelectronic changes, including molecular rearrangements,[13] bandgap shifts,[14] and coordination changes,[15] leading to tunable optical or luminescent properties.

Transition metal complexes offer a unique combination of structural versatility, diverse coordination environments, and enhanced stability, all of which contribute to their chromic behavior.[16] In particular, cyclometalated Pt(II) complexes with multidentate ligands are key stimuli-responsive luminescent materials.[17] The versatile chromic behavior of Pt(II) complexes arises from their rigid square-planar coordination geometry, characteristic of the d^8 platinum center, combined with planar π-conjugated ligands. This structural combination provides access to axial coordination sites, facilitates π–π stacking and Pt···Pt intermolecular interactions, and enables various charge-transfer transitions.[18] These features impart unique optical properties to the complexes in both solution and the solid state, which can be finely tuned through careful ligand selection.

The design of cyclometalating ligands primarily focuses on enhancing luminescent quantum efficiency and tuning emission colors. Our research group has developed several series of phosphorescent cyclometalated platinum(II) complexes incorporating a variety of bidentate and tridentate ligands that feature diazine rings as electron-accepting groups, alongside potential azaheterocyclic auxiliary ligands.[19] These fragments, featuring two non-bonding nitrogen atoms, can coordinate to two metal centers and undergo protonation. Our results demonstrate that incorporating electron-donating or electron-accepting groups into the multidentate and auxiliary ligands effectively tunes and, in some cases, enhances the photophysical properties of these complexes in both solution and the solid state.[20]

We recently adopted a comparative approach focused on a series of cyclometalated Pt(II) complex-based soft salt materials (**S1–9**). These materials consist of two photoactive organometallic complexes with complementary charges, specifically $[Pt(C\text{^}N)(CN)_2]^-$ and $[Pt(C\text{^}N)(en)]^+$ (en = ethane-1,2-diamine), held together by electrostatic attractions and van der Waals forces.[21] This approach has facilitated the elucidation of key structure–property relationships by examining the impact of azaheterocycles (pyridine *vs.* pyrimidine) and the nature and positioning of electron-withdrawing or electron-donating groups on the cyclometalating ligands. Notably, structural modifications to the cyclometalating ligands in both the cationic and anionic platinum(II) complexes of the soft salt series **S1–9** have a pronounced impact on Pt(II)···Pt(II) distances, solid-state emission wavelengths, quantum yields, and chromic behavior. Additionally, the presence of free nitrogen atoms in

[a] *Univ. Rennes, CNRS, ISCR (Institut des Sciences Chimiques de Rennes), UMR 6226, F-35000 Rennes, France. E-mail: sebastien.gauthier@univ-rennes1.fr*
[b] *University of Hradec Králové, Faculty of Science, CZ-500 03 Hradec Králové 3, Czech Republic*
[c] *Universidad de Castilla-La Mancha, Área de Química Orgánica, Facultad de Ciencias y Tecnologías Químicas, Avda. Camilo José Cela 10, 13071, Ciudad Real, Spain*

† Electronic supplementary information (ESI) available. See DOI: https://doi.org/10.1039/d5nj01402f

soft salts containing a C^N pyrimidine-based ligand enables reversible sensitivity to acidic vapors, resulting in phosphorescence quenching. Furthermore, we observed reversible vapochromic behavior in selected soft salts, enabling these novel ion pairs to function as stimuli-responsive materials. Despite improved understanding of the structure–property relationships involving Pt···Pt and π···π interactions, the design of soft salts based on cyclometalated Pt(II) complexes that exhibit high-contrast luminescence remains challenging and continues to attract growing interest.[22,23]

In this study, we explore the preparation, characterization, and optical properties of a novel soft salt, **S** (Fig. 1), comprising two oppositely charged cyclometalated platinum complexes with appropriate C^N ligands. Specifically, the platinum(II) complex $[Pt(C_{Ph_2}\text{^}N)(CN)_2]^-Bu_4N^+$ (**A**), containing a C_{Ph_2}^N bidentate ligand (C_{Ph_2}^N = 2-(4-*N*,*N*-diphenylaminophenyl)-pyridine), was selected as the anionic component. The platinum(II) complex $[Pt(C_{F_2}\text{^}N)(en)]^+Cl^-$ (**C**), incorporating fluorine substitutions and a pyrimidine group on the cyclometalating ligand, was chosen as the cationic component. It is expected that the introduction of fluorine atoms on the cationic component of **S**, in place of the CF_3 group in **S1–9**, will enhance the emission quantum yields in both solution and solid state, as well as improve the chromic responses. In fact, the introduction of electron-withdrawing fluorine atoms onto the phenyl moiety has already been shown to stabilize the highest occupied molecular orbital (HOMO), resulting in a blue shift in emission compared to non-fluorinated compounds and showing an enhanced emission quantum yield in the solid state.[24] The cationic and anionic components were combined to construct the soft salt **S** ($[Pt(C_{F_2}\text{^}N)(en)]^+[Pt(C_{Ph_2}\text{^}N)(CN)_2]^-$) through van der Waals forces and electrostatic interactions. The sensitivity of the emission properties of **S** to various external stimuli was thoroughly investigated and compared to those of analogous compounds. A novel proof-of-concept demonstration of information encryption and decryption using **S** was achieved through thermochromic and vapochromic responses.

Results and discussion

Synthesis and characterization

The cationic platinum(II) complex **C** ($[Pt(C_{Ph_2}\text{^}N)(en)]^+Cl^-$, C_{Ph_2}^N = 2-(2,4-difluorophenyl)pyrimidine) was synthesized in good yield (79%) by stirring the appropriate Pt(II) μ-chloro-bridged dimer complex with ethylenediamine (3 equivalents) in dichloromethane. In contrast, the anionic platinum(II) complex **A** ($[Pt(C_{F_2}\text{^}N)(CN)_2]^-Bu_4N^+$, C_{F_2}^N = 2-(4-*N*,*N*-diphenylaminophenyl)pyridine) was obtained in moderate yield (67%) by stirring the corresponding Pt(II) μ-chloro-bridged dimer complex with tetrabutylammonium cyanide (4 equivalents) in

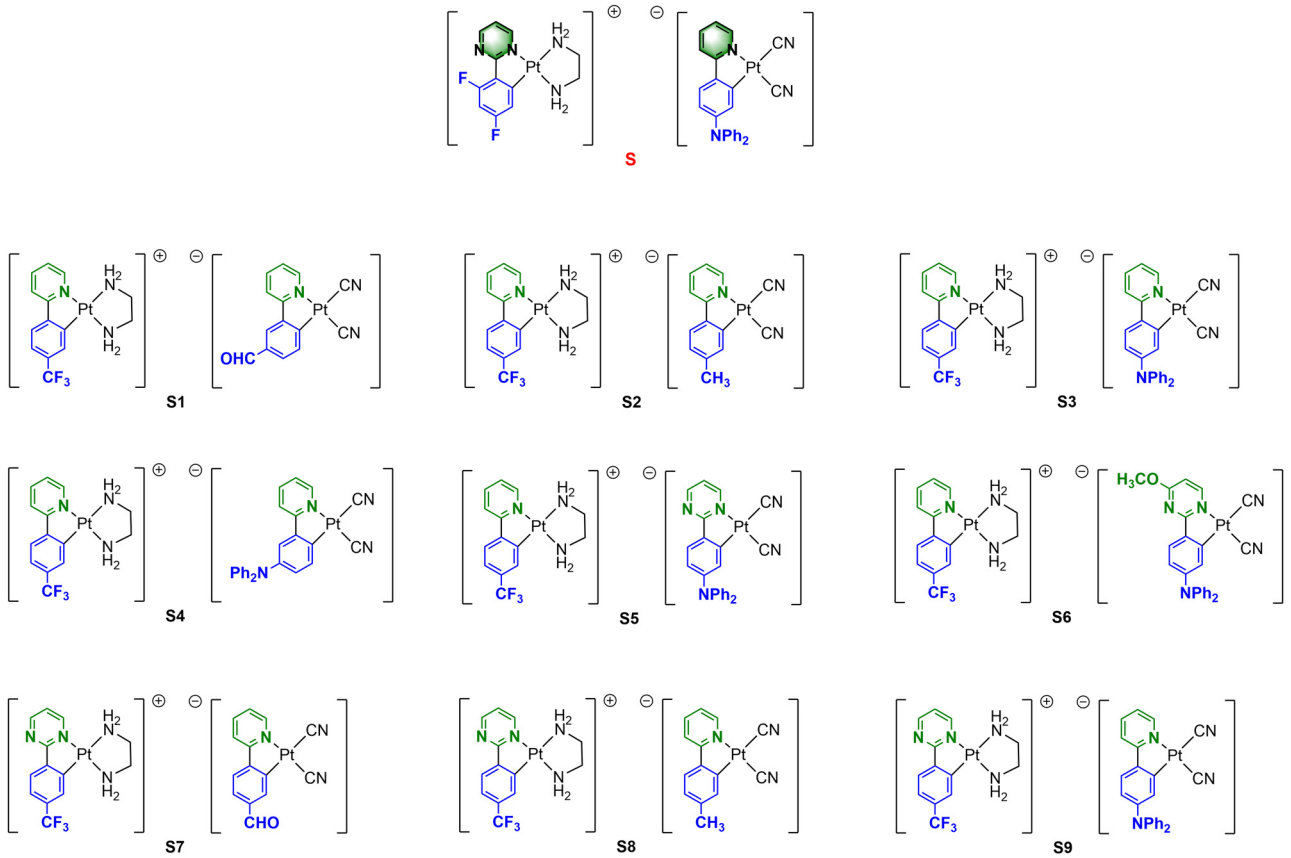

Fig. 1 Molecular structure of the soft salt **S** investigated in this work and previously studied salts **S1–9**.

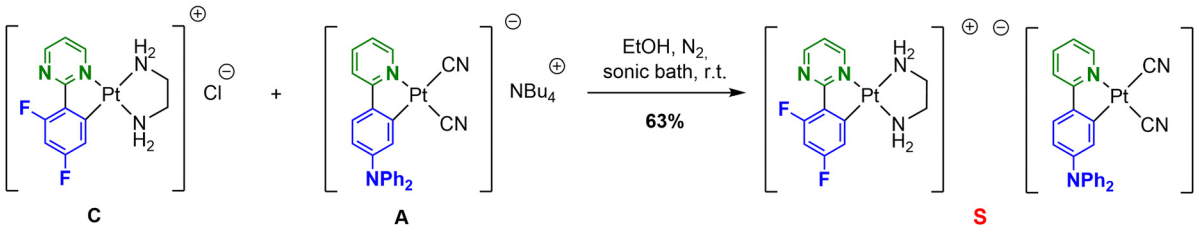

Scheme 1 Synthesis of the soft salt **S**.

dichloromethane at 50 °C (see Scheme S1 in the ESI†).[24b] The soft salt **S** was obtained in a moderate yield (63%) through a metathesis reaction (Scheme 1) by mixing the oppositely charged platinum(II) complexes **A** and **C** in ethanol, using a sonic bath.[21,22d] The ion-paired complex of the soft salt **S** was characterized using electrospray ionization high-resolution mass spectrometry (ESI-HRMS) as well as ^{1}H and ^{13}C nuclear magnetic resonance (NMR) spectroscopy. The characterization data were found to be in full agreement with the proposed structures, as detailed in the SI. Assignments of chemical shifts for the carbon atoms of both molecules were performed using 2D (^{1}H, ^{13}C) COSY, HMQC, and HMBC spectra (Fig. S15–S17, ESI†). Additionally, ^{19}F NMR measurements and 2D (^{1}H–^{19}F and ^{13}C–^{19}F) NMR analyses were performed to assign chemical shifts for carbons bearing fluorine atoms in **C** and **S**, as well as to determine the coupling constants ^{1}J (^{19}F,^{13}C) and ^{4}J (^{19}F,^{19}F) (Fig. S13, S14 and S18, ESI†).

^{15}N NMR spectroscopy is a very useful method to evaluate the effects of complexation on pyridine or pyrimidine group, since the involvement of the nitrogen electron lone pair induces a dramatic deshielding of the ^{15}N RMN signal. The ^{15}N and ^{1}H–^{15}N HMBC NMR spectra (Fig. S19 and S20, ESI†) obtained for **S** allow the assignment of all nitrogen atoms. The chemical shift (δ = −89.9 ppm) for the free nitrogen atom of the pyrimidine moiety is close to the expected value for this heterocycle, while the nitrogen linked to the platinum atom is shielded, with a chemical shift δ = −180.6 ppm, indicating a strong π-donating effect from the metal to the ligand. The same effect is observed for the cyclometalated pyridine of the cationic part (δ = −155 ppm, compared to −63 ppm for the free nitrogen in pyridine).[25] We also observed two distinct signals for the NH_2 groups of ethylenediamine, indicating asymmetry in the coordination to the metal.

Finally, we decided to investigate the ^{195}Pt NMR spectrum for **S** in DMSO-d_6. Two signals at −3447.1 ppm and −4065.2 ppm are observed, confirming the presence of two distinct platinum atoms (Fig. S21, ESI†) with the same chemical shift values as their anionic precursor **A** and cationic precursor **C** (Fig. S22, ESI†). For the anionic Pt complex, the resonance is shifted towards a higher field (−4063.1 ppm), consistent with the σ-donor effect of the CN groups.[26] The ^{195}Pt signal for the cationic complex **C** is detected at −3444.9 ppm, showing a good correlation with the signal detected for **S**.

The thermal stability of **S** was studied using differential scanning calorimetry (DSC), and the corresponding thermograph is presented in Fig. S1 (ESI†). Upon heating the sample initially between 30 and 90 °C, the residual solvents were evaporated, as confirmed by a re-cooling and reheating process, which led to the disappearance of the broad endothermic peak. Further heating induced an irreversible thermal process between 210–260 °C, which may be attributed to a monotropic solid–solid transition or initial decomposition of the sample. The baseline of DSC curve increased significantly up to 300 °C, indicating the gradual exothermic degradation of the sample.

Photophysical properties

The photophysical properties of the soft salt **S** and its precursors were measured in degassed DMSO as well as in the solid state using a KBr matrix (1 wt%), with the data summarized in Table 1 and Fig. 2. In DMSO solution, the absorption spectrum of the soft salt **S** is the superposition of the two precursors **A** and **C** and the emission profiles of **S** and the the anionic precursor **A** are similar, as observed previously for related materials.[21] This suggests that no major interactions occur between the anionic and cationic fragments in solution. For **S** and **A**, the emission profile consists of two bands at 558 and 579 nm attributed to phosphorescence (τ = 10.5 and 23.8 μs respectively) with a shoulder at around 490 nm attributed to ligand centered fluorescence (τ = 3 ns). The photoluminescence

Table 1 Photophysical properties of the soft salt **S** and its precursors **A** and **C** in degassed DMSO solution (10^{-5} M) and in the solid state using KBr matrix (1 wt%)

	DMSO solution			Solid state (KBr matrix, 1 wt%)			
Complex	Absorption λ_{max}/nm (ε/mM^{-1} cm^{-1})	Emission[a] λ_{max}/nm	Φ_{PL}[b] (τ_0/μs)	Emission[a] λ_{max}/nm	Φ_{PL}[c] (τ_0/μs)	k_r/s^{-1}	k_{nr}/s^{-1}
C	340 (3.3)	516	—[d] (—[d])	—[d]	—[d] (—[d])	—[d]	—[d]
A	339 (15.5), 414 (15.6)	558, 579	0.69 (10.5)	545, 579	0.09 (27.5)	3.3×10^3	3.3×10^4
S	338 (19.8), 414 (14.4)	558, 579sh	0.49 (23.8)	658	0.02 (20.15)	1.0×10^3	4.9×10^4

[a] The emission spectra were detected upon excitation at the absorption maxima, λ_{exc} = 340 nm for **C**, and λ_{exc} = 414 nm for **A** and **S**. [b] PLQY (±10%) measured relative to 9,10-bisphenylethynylanthracene in cyclohexane (Φ_{PL} = 1.00).[27] [c] Measured as a powder using an integrating sphere. [d] No emission detected.

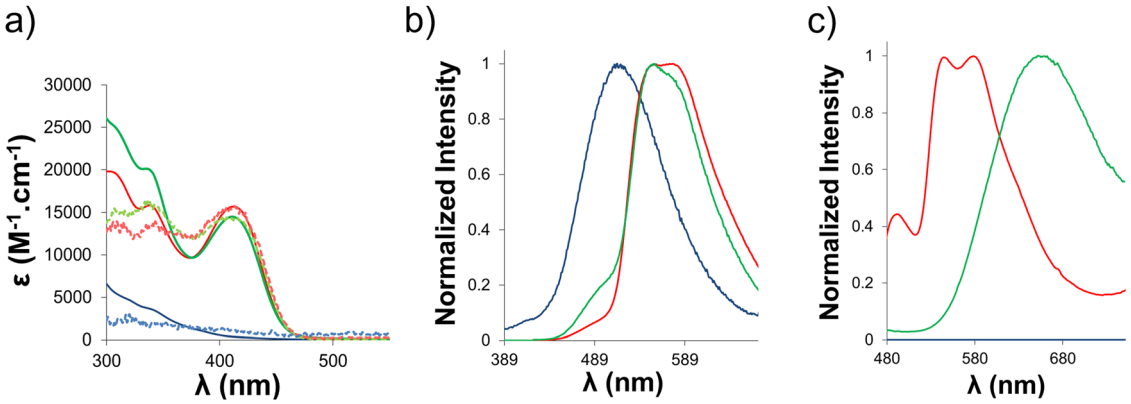

Fig. 2 Normalized absorption (solid line) and excitation (dotted line) spectra (a) and emission spectra (b) of **S** (green, λ_{exc} = 414 nm), **A** (red, λ_{exc} = 414 nm), and **C** (blue, λ_{exc} = 340 nm) in degassed DMSO solution (10^{-5} M). Panel (c) shows the normalized emission spectra of solid samples embedded in a KBr matrix (1 wt%).

quantum yield (PLQY) of **S** in solution, measured at 0.49, is lower than that of **A** (0.69), likely due to electrostatic interactions between the anionic and cationic complexes, which contribute to enhanced emission quenching, even though no emission shift was observed for **S**. However, this value remains significantly higher than that of its analogue **S9** (0.03), which contains a CF_3 group on the cyclometalated ligand of the cationic component.

The effect of aggregation on the photophysical properties was investigated by progressively increasing the water content in a DMSO/water mixture (Fig. 3 and Fig. S2(a), ESI†). Aggregation induced a significant decrease in emission intensity, accompanied by a red-shifted emission band. This phenomenon is attributed to the formation of aggregates and the involvement of a metal–metal-to-ligand charge transfer (MMLCT) excited state.[28] At water content >90%, the emission band is centered around 650 nm, which closely matches the emission band observed in the solid state (λ_{max} = 658 nm).

In the solid state, the red shifted emission of **S** (658 nm) compared to **A** (579 nm) clearly evidence the pairing between cationic and anionic complexes. Surprisingly, **S** exhibits an emission maximum significantly blue-shifted compared to the CF_3-substituted analogue **S9** (695 nm). Additionally, the interaction between the two oppositely charged complexes in **S** is clearly confirmed by the fact that when one equivalent of each precursor, **A** and **C**, is combined in the solid state, the observed emission corresponds to that of complex **A** (Fig. S2(b), ESI†). Indeed, the cationic complex **C** does not exhibit any luminescence. The PLQY of **S** is significantly reduced compared to the solution (0.02 *vs.* 0.49), consistent with the effects of aggregation. Nevertheless, the solid-state emission retains reasonable intensity, allowing the material to be characterized as a dual-state emitter.[29] The emission lifetime in the solid state exceeds 20 μs, indicative of the involvement of a triplet excited state in the emission process.

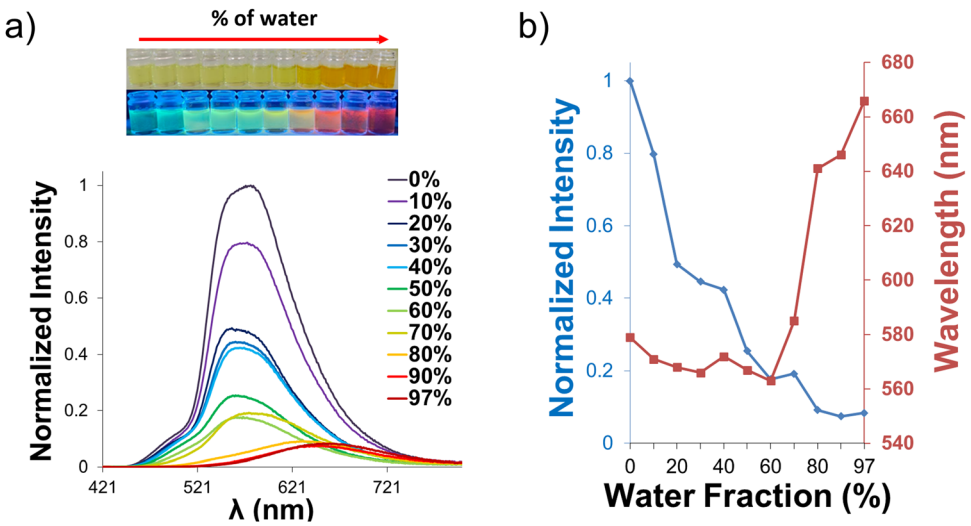

Fig. 3 (a) Emission spectra of **S** (λ_{exc} = 414 nm) in DMSO–water mixtures (10^{-4} M). Above: Photographs of **S** solutions in DMSO–water mixtures with increasing water fractions, taken under UV irradiation, from left to right. (b) Variation of emission intensity and maxima with different water contents.

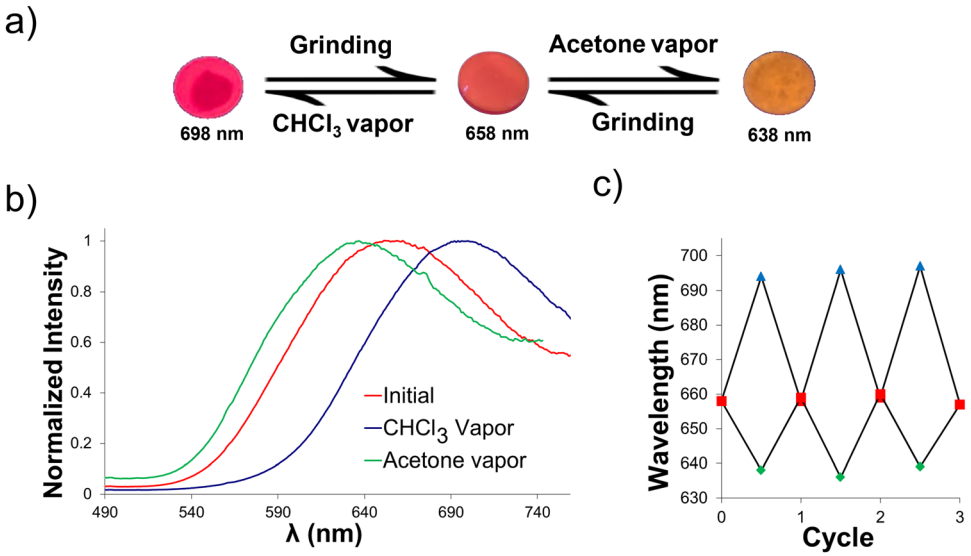

Fig. 4 (a) Photographs of **S** were taken in the dark under irradiation with a handheld UV lamp (λ_{exc} = 365 nm). (b) Effect of solvent ($CHCl_3$ and acetone) fuming and grinding on the emission profile of **S** (λ_{exc} = 414 nm). (c) Emission wavelength variations measured after three repeated cycles of $CHCl_3$ vapor fuming/grinding (blue triangle) or acetone vapor fuming/grinding (green diamond).

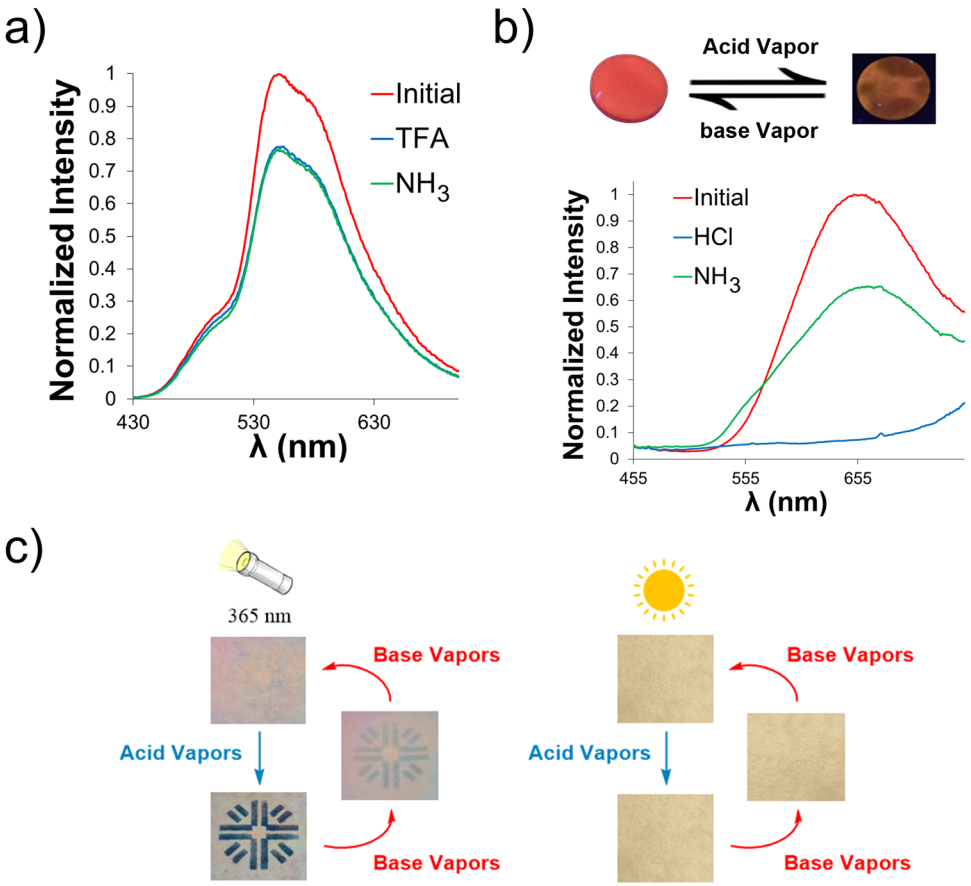

Fig. 5 (a) Emission spectra of **S** in degassed DMSO solution (10^{-5} M) before and after addition of TFA/NH_3 (λ_{exc} = 414 nm). (b) Emission spectra of **S** in the solid state before and after exposure to HCl/NH_3 vapors (λ_{exc} = 414 nm). (c) Photographs of **S** on filter paper under UV-light (λ_{exc} = 365 nm, left) and daylight (right) in the presence of HCl/NH_3 vapors (λ_{exc} = 414 nm).

Response to external stimuli

The effects of various external stimuli on the photophysical properties of **S** were investigated. **S** exhibits vapochromic behavior: $CHCl_3$ and acetone fuming induce red- and blue-shifted emissions, respectively (Fig. 4). In both cases, the initial emission profile can be restored by grinding. Multiple cycles of fuming and grinding can be performed without altering the emission properties. The vapochromic properties of Pt(II) complexes are generally attributed to vapor-induced crystallization, while manual grinding disrupts the framework, restoring the initial emission process.[30]

Many pyrimidine fluorophores have indeed been described as acid sensors.[31] In the case of Pt(II) complexes with pyrimidine-based ligand, the sensitivity to acid vapor is linked to the presence of a free nitrogen atom, not involved in complexation, which is available for interaction with protons. The soft salt **S** does not exhibit the same sensitivity to the presence of acid in solution (Fig. 5(a)) and in the solid state (Fig. 5(b)). In solution, exposure of **S** to TFA results in only a very slight decrease in emission intensity. This phenomenon can be explained by the fact that, in the case of soft salt **S**, the pyrimidine-based ligand is part of the cationic complex, which is non-emissive. Furthermore, even after the addition of ammonia, the initial intensity is not fully recovered. In the solid state, exposure to HCl or TFA vapors results in complete quenching of the emission. This effect is qualitatively reversible upon subsequent exposure to basic ammonia vapors, although the initial emission intensity is not fully recovered. After the first HCl/NH_3 cycle, the reversibility is complete over three cycles. As previously observed with the analogue **S9**, the sensitivity to acid exposure is attributed to the presence of a protonatable pyrimidine-based ligand, even when it is located on the cationic fragment of the soft salt.[21] In the solid state, as previously discussed, the emission is indeed related to the MMLCT excited state, which is influenced by the protonation of the ligand in the cationic component.

A proof-of-concept demonstration of information encryption/decryption is detailed in Fig. 5(c). A filter paper was impregnated with the soft salt **S**, and, using a hollow mask, a portion of the sample representing the logo of the University of Rennes was exposed to HCl vapor. No modification of the sample was observed under daylight, but UV light irradiation (λ_{exc} = 365 nm) revealed the university logo in black. Upon exposure to ammonia vapor, the logo progressively disappeared.

Thermo-induced photoluminescence enhancement was also demonstrated using a sample of **S** impregnated on filter paper. A significant increase in photoluminescence intensity was observed as the temperature was raised to 60 °C (Fig. 6(a)). Upon selective heating through a hollow mask containing the university logo, the logo became visible on the sample under UV light irradiation, while no change in the color of the sample was observed under daylight. This phenomenon is progressively reversible upon cooling over at least three cycles (Fig. 5b and c). For most room-temperature phosphorescent materials, emission quenching is typically observed as the temperature increases.[32] However, the enhancement of emission intensity upon heating could be related to transitioning from an amorphous to crystalline state as reported before.[33]

Conclusion

In summary, we have successfully synthesized and characterized a novel soft salt, **S**, consisting of a pair of ionic Pt(II) complexes bearing specific cyclometalated ligands. We have shown that the cationic and anionic components of **S** interact through electrostatic and van der Waals forces, leading to significant modifications in its luminescent behavior compared to their isolated counterparts and the previously described analogues **S1–9**. The soft salt **S** exhibits photoluminescence in DMSO solution, emitting at 558 nm when excited at 414 nm, with a quantum yield of 0.49. In the solid state, when dispersed in a KBr matrix, a broad emission peak is observed at 658 nm. The study reveals that the complex exhibits vapochromic behavior, with red- and blue-shifted emissions upon exposure to $CHCl_3$ and acetone vapors, respectively. The photoluminescence intensity can be fully restored by grinding, demonstrating the reversibility of the process. **S** exhibits photoluminescence quenching in the presence of acid vapors, with the emission being restored upon exposure to basic ammonia vapors. Additionally, the thermo-induced enhancement of photoluminescence was demonstrated with a

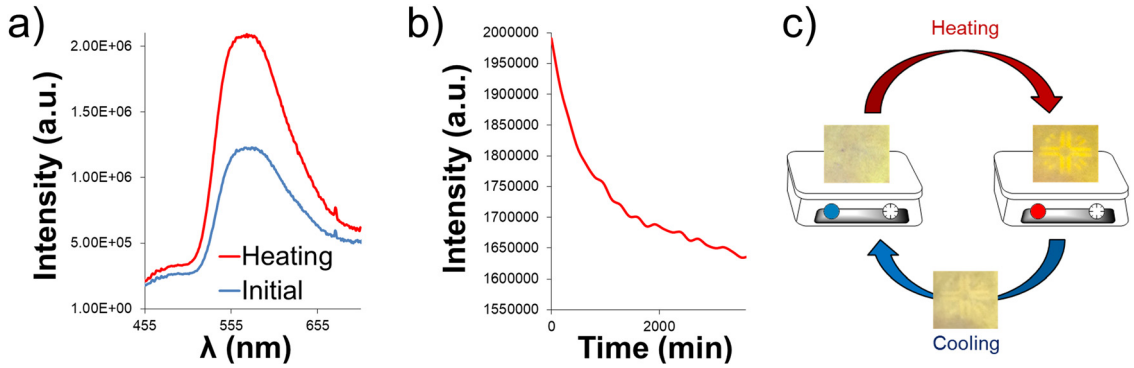

Fig. 6 (a) PL spectrum of **S** on filter paper at room temperature (blue) and after heating to 60 °C (red) (λ_{exc} = 414 nm). (b) Variation in the emission intensity of **S** on filter paper after heating at 60 °C for 3600 s. (c) PL photographs of **S** on filter paper before and after heating and cooling.

sample of **S** impregnated on filter paper. The remarkable sensitivity of **S** to external stimuli, such as solvent vapors, acid/base vapors, and temperature, highlights the versatility and adaptability of cyclometalated Pt(II) complexes, particularly in the context of soft salts. These results pave the way for future research to develop advanced materials with stimuli-responsive properties, offering a wide range of technological applications.

Data availability

The data supporting this article have been included as part of the ESI.†

Conflicts of interest

There are no conflicts to declare.

Acknowledgements

A. R. acknowledges support from Région Bretagne and Conseil Départemental des Côtes d'Armor, France, for his PhD funding (INIMITABLE project). The authors are grateful to the EUR LUMOMAT project and the Investments for the Future program (ANR-18-EURE-0012). A. L. thanks the University of Hradec Králové for financial support. Special thanks are extended to Dr Milan Klikar (University of Pardubice) for performing the DSC analysis.

References

1 (*a*) J. Twilton, C. Le, P. Zhang, M. H. Shaw, R. W. Evans and D. W. C. MacMillan, *Nat. Rev. Chem.*, 2017, **1**, 0052; (*b*) J. He, Z.-Q. Bai, P.-F. Yuan, L.-Z. Wu and Q. Liu, *ACS Catal.*, 2021, **11**, 446–455.

2 (*a*) M. A. Baldo, D. F. O'Brien, Y. You, A. Shoustikov, S. Sibley, M. E. Thompson and S. R. Forrest, *Nature*, 1998, **395**, 151–154; (*b*) S. Lamansky, P. Djurovich, D. Murphy, F. Abdel-Razzaq, H.-E. Lee, C. Adachi, P. E. Burrows, S. R. Forrest and M. E. Thompson, *J. Am. Chem. Soc.*, 2001, **123**, 4304–4312; (*c*) G. Hong, X. Gan, C. Leonhardt, Z. Zhang, J. Seibert, J. M. Busch and S. Bräse, *Adv. Mater.*, 2021, **33**, 2005630.

3 (*a*) M. Irie, T. Fukaminato, T. Sasaki, N. Tamai and T. Kawai, *Nature*, 2002, **420**, 759–760; (*b*) P. Zijlstra, J. W. M. Chon and M. Gu, *Nature*, 2009, **459**, 410–413; (*c*) Q. Gu, J. He, D. Chen, H. Dong, Y. Li, H. Li, Q. Xu and J. Lu, *Adv. Mater.*, 2015, **27**, 5968–5973; (*d*) C.-L. Wong, M. Ng, E. Y.-H. Hong, Y.-C. Wong, M.-Y. Chan and V. W.-W. Yam, *J. Am. Chem. Soc.*, 2020, **142**, 12193–12206.

4 (*a*) J. Xu, P. Yang, M. Sun, H. Bi, B. Liu, D. Yang, S. Gai, F. He and J. Lin, *ACS Nano.*, 2017, **11**, 4133–4144; (*b*) V. W.-W. Yam and A. S.-Y. Law, *Coord. Chem. Rev.*, 2020, **414**, 213298; (*c*) K. K.-W. Lo, *Acc. Chem. Res.*, 2020, **53**, 32–44.

5 (*a*) X. Hou, C. Ke, C. J. Bruns, P. R. McGonigal, R. B. Pettman and J. F. Stoddart, *Nat. Commun.*, 2015, **6**, 6884; (*b*) Z. Li, X. Liu, G. Wang, B. Li, H. Chen, H. Li and Y. Zhao, *Nat. Commun.*, 2021, **12**, 1363; (*c*) A. A. Heider, H. Zhao, Y. Zi, Z. Xu, X. Bai, Y. Cun, Y. Liu, H. Babeker, A. Saeed, Z. Song, J. Qiu, A. Huang, J. Liao and Z. Yang, *Adv. Opt. Mater.*, 2024, **12**, 2002265.

6 (*a*) H. Zou, Y. Hai, H. Ye and L. You, *J. Am. Chem. Soc.*, 2019, **141**, 16344–16353; (*b*) L. M. C. Luong, M. A. Malwitz, V. Moshayedi, M. M. Olmstead and A. L. Balch, *J. Am. Chem. Soc.*, 2020, **142**, 5689–5701.

7 (*a*) C.-Q. Jing, J.-H. Wu, Y.-Y. Cao, H.-X. Che, X.-M. Zhao, M. Yue, Y.-Y. Liao, C.-Y. Yue and X.-W. Lei, *Chem. Commun.*, 2020, **56**, 5925–5928; (*b*) S. Sun, J. Wang, L. Ma, X. Ma and H. Tian, *Angew. Chem., Int. Ed.*, 2021, **60**, 18557–18560; (*c*) B. Deng, Y. Zhu, X. Wang, J. Zhu, M. Liu, M. Liu, Y. He, C. Zhu, C. Zhang and H. Meng, *Adv. Mater.*, 2023, **35**, 2302685.

8 (*a*) G. Huang, Y. Jiang, S. Yang, B. S. Li and B. Z. Tang, *Adv. Funct. Mater.*, 2019, **29**, 1900516; (*b*) Y. Gong, S. He, Y. Li, Z. Li, Q. Liao, Y. Gu, J. Wang, B. Zou, Q. Li and Z. Li, *Adv. Opt. Mater.*, 2020, **8**, 1902036; (*c*) A. E. Norton, M. K. Abdolmaleki, J. Liang, M. Sharma, R. Golsby, A. Zoller, J. A. Krause, W. B. Connick and S. Chatterjee, *Chem. Commun.*, 2020, **56**, 10175–10178.

9 (*a*) J. K. Grey and I. S. Butler, *Coord. Chem. Rev.*, 2001, **219–221**, 713–759; (*b*) J. Zhao, Z. Chi, Y. Zhang, Z. Mao, Z. Yang, E. Ubba and Z. Chi, *J. Mater. Chem.*, 2018, **6**, 6327–6353.

10 (*a*) Z. Li, H. Chen, B. Li, Y. Xie, X. Gong, X. Liu, H. Li and Y. Zhao, *Adv. Sci.*, 2019, **6**, 1901529; (*b*) K. Mutoh, N. Miyashita, K. Arai and J. Abe, *J. Am. Chem. Soc.*, 2019, **141**, 5650–5654; (*c*) Y. Ai, Y. Fei, Z. Shu, Y. Zhu, J. Liu and Y. Li, *Chem. Eng. J.*, 2022, **450**, 138390.

11 (*a*) Y. Ai, Y. Zhu, X. Lei, Y. Zhang, Q. Zeng, Y. Dou, Y. Fei, Z. Shu, J. Xu, H. Xu, J. Liu and Y. Li, *Chem. Eng. J.*, 2023, **465**, 142927; (*b*) T. Sachdeva, S. Gupta and M. D. Milton, *Curr. Org. Chem.*, 2020, **24**, 1976–1998; (*c*) J. Tang, X. Liu, X. Wang, J. Chi, Z. Xiao, Z. Wu and L. Wang, *Inorg. Chem. Front.*, 2024, **11**, 5384–5413.

12 (*a*) J. Chen, Z. Wang, C. Liu, Z. Chen, X. Tang, Q. Wu, S. Zhang, G. Song, S. Cong, Q. Chen and Z. Zhao, *Adv. Mater.*, 2021, **33**, 2007314; (*b*) W. Ma, L. Xu, S. Zhang, G. Li, T. Ma, B. Rao, M. Zhang and G. He, *J. Am. Chem. Soc.*, 2021, **143**, 1590–1597.

13 (*a*) G. Berkovic, V. Krongauz and V. Weiss, *Chem. Rev.*, 2000, **100**, 1741–1754; (*b*) M. Irie, T. Fukaminato, K. Matsuda and S. Kobatake, *Chem. Rev.*, 2014, **114**, 12174–12277; (*c*) Y. Shan, J. Sheng, Q. Zhang, M. C. A. Stuart, D.-H. Qu and N. L. Feringa, *Aggregate*, 2024, **5**, e584; (*d*) X. Zhao, J. Gong, Z. Li, H. H. Y. Sung, I. D. Williams, J. W. Y. Lam, Z. Zhao, B. Z. Tang, W.-Y. Wong and L. Xu, *Aggregate*, 2025, **6**, e686.

14 (*a*) G. Sonmez, C. K. F. Shen, Y. Rubin and F. Wudl, *Angew. Chem., Int. Ed.*, 2004, **43**, 1498–1502; (*b*) B. Sun, X.-F. Liu, X.-Y. Li, Y. Cao, Z. Yan, L. Fu, N. Tang, Q. Wang, X. Shao, D. Yang and H.-L. Zhang, *Angew. Chem., Int. Ed.*, 2020, **59**, 203–208.

15 (*a*) M. Andrzejewski and A. Katrusiak, *J. Phys. Chem. Lett.*, 2017, **8**, 929–935; (*b*) M. Shiga, S. Kawaguchi, M. Fujibayashi,

S. Nishihara, K. Inoue, T. Akutagawa, S.-I. Noro, T. Nakamura and R. Tsunashima, *Dalton Trans.*, 2018, **47**, 7656–7662.

16 (*a*) Z. Chen, Z. Bian and C. Huang, *Adv. Mater.*, 2010, **22**, 1534–1539; (*b*) H. Sasabe, J. Takamatsu, T. Motoyama, S. Watanabe, G. Wagenblast, N. Langer, O. Molt, E. Fuchs, C. Lennartz and J. Kido, *Adv. Mater.*, 2010, **22**, 5003–5007; (*c*) Y. You and W. Nam, *Chem. Soc. Rev.*, 2012, **41**, 7061–7084; (*d*) H. Xiang, J. Cheng, X. Ma, X. Zhou and J. J. Chruma, *Chem. Soc. Rev.*, 2013, **42**, 6128–6185; (*e*) Y. Liu, P. Zhang, X. Fang, G. Wu, S. Chen, Z. Zhang, H. Chao, W. Tan and L. Xu, *Dalton Trans.*, 2017, **46**, 4777–4785; (*f*) T. V. Esipova, H. J. Rivera-Jacquez, B. Weber, A. E. Masunov and S. A. Vinogradov, *J. Am. Chem. Soc.*, 2016, **138**, 15648–15662.

17 (*a*) J. Ni, G. Liu, M. Su, W. Zheng and J. Zhang, *Dyes Pigm.*, 2020, **180**, 108451; (*b*) Q. Zheng, S. Borsley, T. Tu and S. L. Cockroft, *Chem. Commun.*, 2020, **56**, 14705–14708; (*c*) M. A. Soto, V. Carta, M. T. Cano, R. J. Andrews, B. O. Patrick and M. J. MacLachlan, *Inorg. Chem.*, 2022, **61**, 2999–3006.

18 M. A. Soto, R. Kandel and M. J. MacLachlan, *Eur. J. Inorg. Chem.*, 2021, 894–906.

19 (*a*) M. Hruzd, S. Gauthier, J. Boixel, S. Kahlal, N. le Poul, J.-Y. Saillard, S. Achelle and F. R. Le Guen, *Dyes Pigm.*, 2021, **194**, 109622; (*b*) M. Hruzd, N. Le Poul, M. Cordier, S. Kahlal, J.-Y. Saillard, S. Achelle, S. Gauthier and F. R. Le Guen, *Dalton Trans.*, 2022, **51**, 5546–5560; (*c*) M. Hruzd, S. Kahlal, N. Le Poul, L. Wojcik, M. Cordier, J.-Y. Saillard, J. Rodríguez-López, F. R. Le Guen, S. Gauthier and S. Achelle, *Dalton Trans.*, 2023, **52**, 1927–1938; (*d*) M. Fecková, S. Kahlal, T. Roisnel, J.-Y. Saillard, J. Boixel, M. Hruzd, P. le Poul, S. Gauthier, F. Robinle Guen, F. Bureš and S. Achelle, *Eur. J. Inorg. Chem.*, 2021, 1592–1600.

20 M. Hruzd, R. Durand, S. Gauthier, P. le Poul, F. Robinle Guen and S. Achelle, *Chem. Rec.*, 2024, **24**, e202300335.

21 A. Rico, P. le Poul, J. Rodríguez-López, S. Achelle and S. Gauthier, *Dalton Trans.*, 2024, **53**, 11417–11425.

22 (*a*) J. Li, Y. Ma, S. Liu, Z. Mao, Z. Chi, P.-C. Qian and W.-Y. Wong, *Chem. Commun.*, 2020, **56**, 11681–11684; (*b*) J. Li, K. Chen, J. Wei, Y. Ma, R. Zhou, S. Liu, Q. Zhao and W.-Y. Wong, *J. Am. Chem. Soc.*, 2021, **143**, 18317–18324; (*c*) M. Martínez-Junquera, E. Lalinde and M. T. Moreno, *Inorg. Chem.*, 2022, **61**, 10898–10914; (*d*) Y. Ma, K. Chen, J. Lu, J. Shen, C. Ma, S. Liu, Q. Zhao and W.-Y. Wong, *Inorg. Chem.*, 2021, **60**, 7510–7518.

23 (*a*) C. Po, A. Y. Tam, K. M. Wong and V. W. Yam, *J. Am. Chem. Soc.*, 2011, **133**(31), 12136–12143; (*b*) D. Saito, T. Ogawa, M. Yoshida, J. Takayama, S. Hiura, A. Murayama, A. Kobayashi and M. Kato, *Angew. Chem., Int. Ed.*, 2020, **59**(42), 18723–18730; (*c*) M. Yoshida and M. Kato, *Coord. Chem. Rev.*, 2018, **355**, 101–115.

24 (*a*) J. Brooks, Y. Babayan, S. Lamansky, P. I. Djurovich, I. Tsyba, R. Bau and M. E. Thompson, *Inorg. Chem.*, 2002, **41**, 3055–3066; (*b*) A. F. Rausch, U. V. Monkowius, M. Zabel and H. Yersin, *Inorg. Chem.*, 2010, **49**, 7818–7825.

25 W. Städeli and W. Von Philipsborn, *Org. Magn. Reson.*, 1981, **15**, 106–109.

26 J. R. L. Priqueler, I. S. Butler and F. D. Rochon, *Appl. Spectrosc. Rev.*, 2006, **41**, 185–226.

27 M. Taniguchi and J. S. Lindsey, *Photochem. Photobiol.*, 2018, **94**, 290–327.

28 J. Wu, B. Xu, Y. Xu, L. Yue, J. Chen, G. Xie and J. Zhao, *Inorg. Chem.*, 2023, **62**, 19142–19152.

29 (*a*) J. L. Belmonte-Vázquez, Y. A. Amador-Sánchez, L. A. Rodríguez-Cortés and B. Rodríguez-Molina, *Chem. Mater.*, 2021, **33**, 7160–7184; (*b*) A. Huber, J. Dubbert, T. D. Scherz and J. Voskuhl, *Chem. – Eur. J.*, 2023, **29**, e202202481.

30 (*a*) M. Kato, *IUCrJ*, 2024, **11**, 442–452; (*b*) K. Ishii, S. Takanohashi, M. Karasawa, K. Enomoto, Y. Shigeta and M. Kato, *J. Phys. Chem. C*, 2021, **125**, 21055–21061; (*c*) Y. Shigeta, A. Kobayashi, T. Ohba, M. Yoshida, T. Matsumoto, H.-C. Chang and M. Kato, *Chem. – Eur. J.*, 2016, **22**, 2682–2690; (*d*) M. Kato, S. Kishi, Y. Wakamatsu, Y. Sugi, Y. Osamura, T. Koshiyama and M. Hasegawa, *Chem. Lett.*, 2005, **34**, 1368–1369.

31 (*a*) S. Achelle, J. Rodríguez-López, F. Bureš and F. Robinle Guen, *Chem. Rec.*, 2020, **20**, 440–451; (*b*) F. Kournoutas, I. K. Kalis, M. Fecková, S. Achelle and M. Fakis, *J. Photochem. Photobiol., A*, 2020, **391**, 112398.

32 J.-A. Li, Z. Song, Y. Chen, C. Xu, S. Li, Q. Peng, G. Shi, C. Liu, S. Luo, F. Sun, Z. Zhao, Z. Chi, Y. Zhang and B. Xu, *Chem. Eng. J.*, 2021, **418**, 129167.

33 (*a*) H. Wang, H. Ma, N. Gan, K. Qin, Z. Song, A. Lv, K. Wang, W. Ye, X. Yao, C. Zhou, X. Wang, Z. Zhou, S. Yang, L. Yang, C. Bo, H. Shi, F. Huo, G. Li, W. Huang and Z. An, *Nat. Commun.*, 2024, **15**, 2134; (*b*) X. W. Liu, W. Zhao, Y. Wu, Z. Meng, Z. He, X. Qi, Y. Ren, Z.-Q. Yu and B. Z. Tang, *Nat. Commun.*, 2022, **13**, 3887.